



ELSEVIER

NeuroImage

www.elsevier.com/locate/ynimg
NeuroImage xx (2007) xxx–xxx

Structural correlates of psychopathological symptom dimensions in schizophrenia: A voxel-based morphometric study

Nikolaos Koutsouleris,^{a,1} Christian Gaser,^{b,1} Markus Jäger,^a Ronald Bottlender,^a Thomas Frodl,^a Silvia Holzinger,^a Gisela J.E Schmitt,^a Thomas Zetzsche,^a Bernhard Burgermeister,^a Johanna Scheuerecker,^a Christine Born,^c Maximilian Reiser,^c Hans-Jürgen Möller,^a and Eva M. Meisenzahl^{a,*}

^aDepartment of Psychiatry and Psychotherapy, Ludwig-Maximilians-University, Nussbaumstr, 7, 80336 Munich, Germany

^bDepartment of Psychiatry, Friedrich-Schiller-University, Jena, Germany

^cDepartment of Radiology, Ludwig-Maximilians-University, Munich, Germany

Received 26 July 2007; revised 24 September 2007; accepted 17 October 2007

Structural neuroimaging has substantially advanced the neurobiological research of schizophrenia by describing a range of focal brain alterations as possible neuroanatomical underpinnings of the disease. Despite this progress, a considerable heterogeneity of structural findings persists that may reflect the phenomenological diversity of schizophrenia. It is unclear whether the range of possible clinical disease manifestations relates to a core structural brain deficit or to distinct structural correlates. Therefore, gray matter density (GMD) differences between 175 schizophrenic patients (SZ) and 177 matched healthy control subjects (HC) were examined in a three-step approach using cross-sectional and conjunctive voxel-based morphometry (VBM): (1) analysis of structural alterations irrespective of symptomatology; (2) subdivision of the patient sample according to a three-dimensional factor model of the PANSS and investigation of structural differences between these subsamples and healthy controls; (3) analysis of a common pattern of structural alterations present in all patient subsamples compared to healthy controls. Significant GMD reductions in patients compared to controls were identified within the prefrontal, limbic, paralimbic, temporal and thalamic regions. The disorganized symptom dimension was associated with bilateral alterations in temporal, insular and medial prefrontal cortices. Positive symptoms were associated with left-pronounced alterations in perisylvian regions and extended thalamic GMD losses. Negative symptoms were linked to the most extended alterations within orbitofrontal, medial prefrontal, lateral prefrontal and temporal cortices as well as limbic and subcortical structures. Thus, structural heterogeneity in schizophrenia may relate to specific patterns of GMD reductions that possibly share a common prefrontal-perisylvian pattern of structural brain alterations. © 2007 Elsevier Inc. All rights reserved.

Introduction

Over the last decade, neuroimaging revealed a growing number of structurally altered brain regions in schizophrenic patients. Recent meta-analyses (Honea et al., 2005; Wright et al., 2000) identified the main foci of these alterations in frontal, temporal and limbic regions as well as the ventricular system. Despite this substantial progress, evidence for neuroanatomical abnormalities remains considerably heterogeneous.

The debate about structural heterogeneity in schizophrenia has been inspired by the disease's psychopathological diversity and has contributed to many different disease models, representing either a more "monistic" or "pluralistic" neurobiological perspective. One important concept is the hypothesis of a single, unifying pathophysiological process that underlies different disease phenotypes. Based on this concept, Andreasen (1999) integrated the diverse clinical phenomenology into the heuristic model of "cognitive dysmetria" by suggesting a disruption of the cortico-cerebellar-thalamo-cortical circuit (CCTCC) as the main cause for the disassociation of mental activity. This model has received support from previous MRI studies of schizophrenic patients that detected alterations in the three key nodes (prefrontal cortex, thalamus, cerebellum) of the CCTCC (Schlösser et al., 2003; Volz et al., 2000; Gaser et al., 1999).

Beside these brain regions, further structural alterations were identified in the temporal, limbic and paralimbic areas of schizophrenic patients by means of Region-of-Interest (ROI) techniques (Shenton et al., 2001; Wright et al., 2000). Recently, whole-brain VBM and deformation-based morphometric studies (Davatzikos et al., 2005; Gaser et al., 2004, 1999; Hulshoff Pol et al., 2001) confirmed and extended these findings, thus providing an insight into the complex, distributional nature of cortical alterations involved in the neurobiology of the disorder. These results may strengthen the hypothesis of a core fronto-temporo-limbic

* Corresponding author.

E-mail address: Eva.Meisenzahl@med.uni-muenchen.de (E.M. Meisenzahl).

¹ Both authors contributed equally to this work.

Available online on ScienceDirect (www.sciencedirect.com).

disconnectivity as the neural substrate of the diverse schizophrenic symptomatology.

In contrast to these models, the “pluralistic” perspective suggests that the broad clinical syndrome of schizophrenia is subdivided into different nosological entities. Carpenter et al. (1988) identified a “separate disease” within the syndrome of schizophrenia characterized by enduring negative and less severe positive symptoms. Sigmundsson et al. (2001) applied the VBM methodology to a homogeneous sample of schizophrenic patients selected for these “deficit symptoms” and identified two clusters of left-lateralized GMD reductions in the perisylvian/opercular and the medial temporal region, as well as bilateral reductions in the medial prefrontal cortices.

Exploring the associations between clinical phenotypes and the underlying neurobiology may be an appropriate strategy for testing the validity of these different disease models. In this context, several authors observed correlations between positive symptoms and morphometric alterations in the orbitofrontal cortex, the insula, the temporal pole and superior temporal gyrus using ROI or VBM techniques (Makris et al., 2006; Pressler et al., 2005; Gaser et al., 2004; Crespo-Facorro et al., 2004, 2000; Matsumoto et al., 2001; Flaum et al., 1995). Associations between disorganized symptoms and volume reductions have been described for the amygdala–hippocampus–complex (AHC), the parahippocampus and the STG (Suzuki et al., 2005; Rajarethinam et al., 2001; Shenton et al., 1992). Interestingly, many of these cortical structures belong to the “paralimbic brain”—a higher-order, multimodal association network potentially involved in the pathophysiology of schizophrenia (Mesulam and Mufson, 1986).

A sensible strategy to study the links between psychopathology and neurobiology assumes that specific pathophysiological processes are associated with clusters of psychopathological items, that can be described as patterns of co-occurring symptoms revealed by means of factor analysis. This technique has been consistently applied in order to study the phenotypical heterogeneity of schizophrenia. Using factor analysis of the PANSS and SANS/SAPS scales, a large number of studies have provided strong evidence for a dimensional model of schizophrenic psychopathology with (at least) three symptom dimensions (Grube et al., 1998).

In contrast to earlier phenomenological distinctions of paranoid, hebephrenic or katatonic schizophrenia, factorial models emphasize that different symptom dimensions are independent, but also share overlapping clinical features, and, therefore, may not be regarded as clinical subtypes or syndromes of the disease (Andreasen et al., 1995). These models enabled researchers to study the relationships between specific symptom constellations and their underlying neural substrates. However, up to now only few authors (Pressler et al., 2005; Crespo-Facorro et al., 2004; Flaum et al., 1995) have applied this promising approach to structural neuroimaging in schizophrenia. First, Flaum et al. (1995) described associations between ventricular and temporal lobe volumes and positive and negative symptom clusters derived from a three-factor model of the SANS/SAPS consisting of negative, positive and disorganized symptom dimensions (Arndt et al., 1991).

Based on a factorial model of schizophrenic psychopathology, the present VBM study explored the phenotypical and structural heterogeneity of schizophrenia by examining the associations between different symptom dimensions and possible underlying structural brain correlates in a large, cross-sectionally recruited database of patients compared to matched healthy controls. The

following hypotheses were tested: (1) Different symptom dimensions relate to selective patterns of structural brain alterations: negative symptoms may be linked to prominent alterations of the fronto-temporo-limbic system. Positive symptoms may be associated with left-hemispheric alterations of the frontal and perisylvian structures, the limbic system and the thalamus, whereas disorganized symptoms may relate to alterations of the temporal, paralimbic and limbic structures. (2) A significant overlap between these patterns exists, possibly representing a core neurobiological substrate of *all* symptom dimensions. Therefore, a three-step approach was implemented. First, structural alterations were examined irrespective of symptomatology in the entire patient sample compared to healthy volunteers. Secondly, a factor analysis was employed for dividing the patients into three subsamples according to the prevailing individual symptom dimension. Structural alterations were examined within these subsamples compared to healthy controls. Thirdly, a conjunctive VBM analysis was performed in order to evaluate possible core alterations across all subsamples.

Methods

Subjects

One hundred seventy-five patients with the DSM-IV diagnosis of schizophrenia from the Department of Psychiatry and Psychotherapy at Ludwig-Maximilians University, Munich, Germany and 177 healthy controls matched for age, gender and handedness participated in this study (Table 1). No statistical differences were observed between both samples concerning age, gender and handedness. As expected, SZ had significantly less educational years than HC.

All participants provided their written informed consent prior to MRI and clinical examination. Patient recruitment was performed by trained clinical investigators and consisted of a Structured Clinical Interview for DSM-IV-Axis I Disorders (SCID-I), a standardized clinical interview for the assessment of medical and psychiatric history, the review of patients’ records and the evaluation of disease severity and psychopathology by means of the PANSS (Kay et al., 1987). A consensus diagnosis of schizophrenia was achieved by two experienced psychiatrists based on the DSM-IV criteria and the SCID. Age of disease onset was defined retrospectively as the first time patients experienced psychotic symptoms in the context of a general decline in social and cognitive functioning as reported by the first physician or psychologist in charge. The interval between age of disease onset and the first reported prescription of antipsychotic agents defined duration of untreated psychosis. For every patient, the dose of antipsychotic agents at scan time was converted to chlorpromazine equivalents (CPZ-eq) (Lambert et al., 2004). One hundred fifty-three patients received at least one neuroleptic agent, with a mean (SD) of 316.7 (351.5) mg CPZ-eq (Table 1). The most commonly prescribed antipsychotics were risperidone, haloperidole, clozapine, amisulpride, olanzapine, perazine, pimozide and flupentixole.

Exclusion criteria were other psychiatric and/or neurological diseases, past or present regular alcohol abuse and/or consumption of illicit drugs as reported by the study participants, their relatives and/or the patients’ records, as well as past head trauma with loss of consciousness or electro-convulsive treatment. HC with a positive familial history for mental illnesses (1st degree relatives) were also excluded.

Table 1

Statistical analysis of sociodemographic, clinical and global anatomical parameters of HC and the entire SZ group, as well as of the three factor subgroups SZ-NEG, SZ-POS and SZ-DIS

Variable	Whole groups				Factor subgroups				
	HC	SZ	T/χ^2	p	SZ-NEG	SZ-POS	SZ-DIS	F/χ^2	p
<i>Sociodemographic</i>									
<i>N</i>	177	175			59	61	55		
Age at scan (SD)	31.5 (9.2)	31.7 (10.2)	-0.21	0.836	32.8 (10.3)	32.7 (9.9)	29.4 (10.2)	2.06	0.131
Gender (male/female)	123/54	130/45	1.00	0.317	50/9	43/18	37/18	5.26	0.072
Handedness (right/left/ambi)	164/12/1	162/11/2	0.38	0.828	58/1/0	55/5/1	49/5/1	4.37	0.359
Educational years (SD)	11.6 (1.7)	10.5 (2.1)	5.08	0.000*	10.6 (1.9)	10.6 (2.2)	10.4 (2.2)	0.35	0.709
<i>Clinical</i>									
Age of disease onset (SD)		27.4 (9.7)			25.5 (9.6)	30.5 (10.6)	26.3 (7.9)	4.58	0.012*
Duration of untreated psychosis (SD)		1.6 (2.5)			1.9 (2.7)	1.6 (2.8)	1.1 (2.1)	1.18	0.312
CPZ-eq at scan (SD) (mg)		316.7 (351.5)			372.8 (377.3)	315.2 (343.8)	256.5 (326.4)	1.42	0.246
No antipsychotic		24			6	12	6	8.14	0.228
≥ 1 typical antipsychotic		41			12	13	16		
≥ 1 atypical antipsychotic		97			33	33	31		
≥ 1 both		3			8	3	2		
PANSS sum score (SD)		83.3 (28.8)			80.1 (18.8)	90.0 (35.4)	79.3 (28.4)	2.61	0.077
PANSS positive score (SD)		19.0 (7.8)			13.0 (4.7)	24.4 (8.0)	19.2 (5.3)	49.44	0.000*
PANSS negative score (SD)		22.3 (9.8)			26.6 (7.4)	19.0 (9.7)	21.5 (10.5)	10.32	0.000*
PANSS general score (SD)		42.0 (16.2)			40.3 (10.1)	46.6 (19.7)	38.7 (16.4)	4.04	0.019*
<i>Global brain volumes (mm³)</i>									
Gray matter volume (SD)	632.7 (81.2)	610.5 (80.5)	2.58	0.010*	613.8 (73.0)	591.8 (87.3)	627.7 (77.2)	3.02	0.052
White matter volume (SD)	534.6 (65.7)	531.5 (61.3)	0.46	0.650	544.5 (52.6)	524.1 (68.9)	525.8 (59.9)	2.03	0.134
Cerebro-spinal fluid (SD)	485.7 (93.2)	521.7 (100.7)	-3.48	0.001*	539.2 (89.0)	516.5 (106.2)	508.6 (105.3)	1.45	0.238
Total intracranial volume (SD)	1653.0 (181.7)	1663.7 (171.0)	-0.57	0.571	1697.5 (143.7)	1632.4 (193.7)	1662.1 (167.5)	2.21	0.113
Squared distance to mean voxel value in GMD (SD) * 10 ³	4.4 (2.2)	4.2 (2.5)	0.62	0.537	4.0 (1.7)	4.4 (3.3)	4.0 (2.1)	0.59	0.555

Significance threshold defined at $p < 0.05$. Abbreviations: ambi, ambidextruous; T , T value of Student's t test; F , F value of one-way analysis of variance; χ^2 , Pearson's χ^2 -test; CPZ-eq, chlorpromazine equivalents.

Psychopathology and factor analysis

Psychopathological symptoms were assessed by trained clinical investigators using the PANSS at scan time (Table 1). Using the R software package (R Project for Statistical Computing), the patterns of co-occurring symptoms were analyzed by employing a maximum-likelihood factor analysis on the PANSS items using three, four and five factor models. As symptom dimensions might be correlated, the oblique PROMAX rotation method was used. The three-dimensional model consisting of a negative, positive and disorganized symptom dimension was chosen for subsequent VBM analysis (see Discussion). The internal consistency of symptom factors was measured by Cronbach's α and inter-factor correlations were calculated. Every SZ was assigned to one of the three symptom dimensions according the maximum individual factor score (Supplementary Fig. 12), resulting in a negative (SZ-NEG), positive (SZ-POS) and disorganized factor (SZ-DIS) sample.

MRI data acquisition

MR images were obtained on a 1.5 T Magnetom Vision scanner (Siemens, Erlangen, Germany). Subjects were scanned with a T1-weighted 3D-MPRAGE sequence (TR, 11.6 ms; TE, 4.9 ms; field of view, 230 mm; matrix, 512 × 512; 126 contiguous axial slices of 1.5 mm thickness; voxel size, 0.45 × 0.45 × 1.5 mm). Data analysis was performed using the VBM2 toolbox (<http://dbm.neuro.uni->

jena.de), an extension of the SPM2 package (Wellcome Department of Cognitive Neurology, London, UK).

MRI data preprocessing

The VBM2 toolbox implementing the optimized VBM approach (Good et al., 2001) was used for data preprocessing. Optimized VBM consists of a two-step procedure starting with the construction of a study-specific, whole brain template and tissue priors accounting for the magnetic field properties of the scanner as well as for the anatomical properties of the study cohorts. In the second step, the customized template and tissue priors were used for data segmentation, registration to and re-segmentation in standard space. Thus, inter-subject global brain size differences were removed and homologous brain regions were brought into alignment.

The VBM2 toolbox extends the existing optimized VBM algorithms as it increases the quality of segmentation by applying a Hidden Markov Field (HMRF) model (Bach Cuadra et al., 2005) to the segmented tissue classes at both steps of the protocol. The HMRF algorithm provides spatial constraints based on neighboring voxel intensities within a 3 × 3 × 3 voxel cube. It removes isolated voxels which are unlikely to be a member of a certain tissue class and also closes holes in a cluster of connected voxels of a certain class resulting in a higher signal-to-noise ratio of the final tissue probability maps. In this study, only gray matter density (GMD) maps were used for statistical analysis after smoothing with a 12 mm FWHM Gaussian kernel.

Additional calculations were performed using the “Tools” algorithms of the VBM2 toolbox: Global gray matter, white matter and CSF volumes as well as total intracranial volumes were computed for the HC and the entire SZ group, as well as for the factor samples. Anatomical homogeneity in each factor sample was assessed by calculating the squared distances to the mean voxel value of the individual GMD maps (Table 1).

Statistical analysis

Within the framework of the General Linear Model, a univariate analysis of variance between HC and SZ samples was performed. Effects of age and gender on brain structure were modeled as covariates of no interest (Supplementary Fig. 1). As normalization to standard space removed the effects of global brain volume differences in the GMD maps, this parameter was not entered as nuisance variable in the statistical design. After parameter estimation, group differences were assessed using Gaussian Random Field theory. False positive errors were minimized by a family-wise error-corrected (FWE) height threshold of $P < 0.05$. Significant, suprathreshold voxels and local maxima were assigned to anatomical regions by means of Automated Anatomical Labeling (Tzourio-Mazoyer et al., 2002).

In the first step of the analysis, two T contrasts were constructed in order to examine regional GMD increases/decreases between the HC and entire SZ group (Supplementary Fig. 1). Secondly, significant GMD increments/decrements were assessed between HC and the three PANSS factor samples, respectively. The effect size of significant regional GMD differences was quantified using Cohen's d (Supplementary Figs. 3–5). Additionally, *between-factor* differences were computed by calculating the percental difference maps for the contrast images of the factor sample comparisons (Supplementary Fig. 6). Thirdly, a conjunctive VBM analysis was performed using the T contrasts of the second analysis step. Conjunction enables inferences about one or more effects across study populations (Friston et al., 2005). We were interested in the conjunction that *all* three subsamples showed significant GMD reductions compared to HC.

In an additional VBM analysis, factor samples were dichotomized into “high” and “low loading” subsamples using the median split of the individual factor scores. The rationale of this analysis was to test the hypothesis that factor subsamples consisting of high loaders show larger anatomical differences compared to low loaders. This analysis was reported as supplementary material (Supplementary Figs. 9–11).

Finally, effects of age of onset and medication at scan (CPZ-eq) on brain structure were assessed in supplementary VBM analyses. Therefore, reduced statistical designs were constructed containing only the data of the SZ subsamples and the respective parameters as covariates of interest. F tests were performed at $P < 0.001$, uncorrected.

Results

Factor analysis

Factor analysis provided a three-, four- and five-factor model of the PANSS explaining a cumulative variance of 51%, 53% and 56% in the data. The three-factor model gave factor sample sizes of $N_{1,2,3} = 59, 61, 55$. The four-factor model produced $N_{1,2,3,4} = 35, 47, 31, 62$ and the five-factor solution resulted in $N_{1,2,3,4,5} = 27, 32, 26,$

45, 45. The three-dimensional model was chosen for subsequent analysis (see Discussion). The highest factor loadings in the first, “negative” factor were attained by “emotional withdrawal”, “passive/apathetic social withdrawal” and “blunted affect” (Table 2). In the second, “positive” factor “hostility”, “guilt feelings” and “suspiciousness/persecution” obtained highest loadings. In the third, “disorganized” factor, the maximum loadings were reached by “conceptual disorganization”, “poor attention” and “disorientation”. The

Table 2

Results of exploratory maximum-likelihood factor analysis of the data of 175 SZ: factor loadings of PANSS items and cumulative variance (CumVar) explained by three extracted factors F1, F2 and F3

Item	Loadings			Description
	F1	F2	F3	
<i>Factor 1</i>				
N2	0.987			Emotional withdrawal
N4	0.951	−0.189		Passive/apathetic social withdrawal
N1	0.899	−0.225		Blunted affect
G16	0.856	0.226	−0.238	Active social avoidance
G15	0.765	0.358	−0.247	Preoccupation
G13	0.709	−0.213		Disturbance of volition
N3	0.696	0.255		Poor rapport
G6	0.563	0.254	−0.323	Depression
G7	0.504	0.200	0.214	Motor retardation
N6	0.449	0.419		Lack of spontaneity and flow of conversation
N7	0.441	0.319		Stereotyped thinking
<i>Factor 2</i>				
P7		0.768		Hostility
G3		0.761		Guilt feelings
P6	−0.238	0.741		Suspiciousness/persecution
P4	−0.237	0.701	0.182	Excitement
P5		0.690		Grandiosity
G9	0.204	0.675		Unusual thought content
P1	−0.432	0.660		Delusions
G14	0.136	0.648		Poor impulse control
G2		0.646		Anxiety
G4		0.622	0.108	Tension
G1	0.170	0.615		Somatic concern
G5	0.170	0.562	0.155	Mannerisms and posturing
N5	0.293	0.448		Difficulty in abstract thinking
G8	0.174	0.399	0.275	Uncooperativeness
P3	−0.240	0.396		Hallucinatory behaviour
<i>Factor 3</i>				
P2	−0.305	0.255	0.729	Conceptual disorganization
G11		0.139	0.607	Poor attention
G10		0.387	0.389	Disorientation
G12			0.205	Lack of judgement and insight
CumVar	0.22	0.44	0.51	
Chronbach's α	0.93	0.91	0.64	
<i>Factor correlation matrix</i>				
F1	1.000	0.396	0.396	
F2	0.396	1.000	0.543	
F3	0.396	0.543	1.000	

internal consistencies of the negative, positive and disorganized symptom dimensions were $\alpha=0.93$, 0.91 and 0.64 (Table 2). Factor samples did not differ significantly regarding age at scan, educational years, handedness, duration of untreated psychosis, type of medication (no medication, typical, atypical, both), dose (CPZ-eq) at time of scan and anatomical sample homogeneity (Table 1). Trend differences were found in SZ-NEG regarding global gray matter volume and gender distribution. Age of disease onset was significantly different between factor samples.

VBM analysis of HC versus SZ

GMD reductions were identified in frontal, temporal, parietal and limbic structures in 175 SZ compared to 177 HC (Fig. 1). Large clusters of reductions were found bilaterally in the perisylvian regions comprising insula, temporal poles, STG, supramarginal and inferior frontal gyri. Reductions extended to the lateral orbitofrontal, middle, superior frontal and inferior parietal gyri, as well as to the middle, inferior temporal and fusiform gyri. The frontal interhemispheric region showed reductions within the medial orbitofrontal, anterior cingulate (ACC) and dorsomedial prefrontal cortex. Further reductions were identified in limbic, occipital, subcortical and cerebellar structures. No significant GMD increases were observed in this or the following analyses.

VBM analysis of HC versus SZ factor samples

HC versus SZ-NEG

This sample showed the most extended GMD reductions (Figs. 2 and 3) and largest effect sizes (Supplementary Fig. 3) of all factor samples. Bilateral reductions were mainly located in five cortical areas: the frontal interhemispheric region (subgenual cortex, ACC), the perisylvian regions (Rolandic operculum, insula, STG, supramarginal and inferior frontal gyri), the lateral frontal cortices, the lateral and inferior temporal structures and the limbic lobe.

HC versus SZ-POS

This sample showed GMD reductions within the left perisylvian region and the left medial orbitofrontal, the lateral prefrontal cortex and the thalamus bilaterally (Figs. 2 and 3). Reductions within the left STG and supramarginal gyrus as well as the thalamus were larger, the prefrontal clusters were smaller compared to SZ-NEG. In contrast to SZ-NEG, no reductions were observed in limbic structures. The largest effect sizes (range: 0.5 – 0.7) were observed predominantly on the left hemisphere within the STG, the anterior insula and the ventrolateral and dorsolateral prefrontal cortex (Supplementary Fig. 4).

HC versus SZ-DIS

This sample showed GMD reductions in three cortical areas (Figs. 2 and 3): the perisylvian regions (*bilateral*: anterior insula, posterior STG, inferior frontal, supramarginal gyri; *left hemisphere*: temporal pole, anterior STG), the medial orbitofrontal cortices, bilaterally and the left limbic system (amygdala). The effect sizes in these areas ranged between 0.5 and 0.7 . The GMD reductions overlapped with, but did not reach the extent of GMD alterations in SZ-NEG. In contrast to SZ-POS, the perisylvian reductions were mainly bilaterally localized. Additional alterations were observed in the lateral and inferior temporal structures.

Conjunctional VBM analysis

GMD reductions across all PANSS factor groups occupied mainly three cortical areas and the thalamus (Supplementary Fig. 7 and 8): (1) bilateral perisylvian clusters (Insula, Rolandic operculum, inferior frontal, supramarginal gyri, STG, temporo-polar cortex); (2) left-hemispheric clusters in the middle and inferior temporal cortex; (3) bilateral clusters within the orbitofrontal areas, the medial prefrontal cortices, the ACC and the lateral prefrontal regions.

Supplementary analysis

No significant interactions between GMD, age of onset or medication dose were observed in the factor samples.

Discussion

Factor analysis

The three-dimensional factor model of the PANSS was consistent with well established previous models identifying a negative, positive and disorganized symptom dimension of schizophrenic psychopathology with a variety of symptom scales (review by Grube et al., 1998). Recent factor-analytic studies reported that pentagonal models and even hexagonal models may better account for the dimensional structure of the PANSS compared to earlier three-dimensional models (Van den Oord et al., 2006). However, we refrained from employing our tetra- or pentagonal models for the subsequent VBM analysis as they accounted only for small additional increases in variance information and because they produced significantly smaller and unequally sized factor samples. Nevertheless, these analyses should be conducted with significantly larger sample sizes in the future.

Methodological criticism may concern the categorization of patients into factor samples according to their maximum factor scores. This approach may introduce artificial boundaries within a spectrum of coexisting and overlapping symptom dimensions. Therefore, a regression analysis of factor loadings and VBM data may better model the dimensional structure and possible overlaps between different symptom components. However, this approach excludes a healthy reference group for whom no psychopathological data are available. Moreover, it is limited to the analysis of linear relations between the variables of interest. In contrast, the favored approach allowed for higher degrees of freedom necessary for the detection of subtle structural differences associated with the three symptom dimensions.

Due to our cross-sectional study design, the described symptom dimensions were derived only from a cutout of the individual courses of our patients. Psychopathology may vary intra-individually over time and it is therefore necessary to discuss the results of this study in the light of the dynamics of psychopathological pattern changes. Using longitudinal factor analysis in a prospective, 2-year follow-up study, Arndt et al. (1995) reported that the three symptom dimensions observed at baseline tended to “change in unison and independently from one another”. Similarly, Van der Does et al. (1995) showed that their four-dimensional factorial symptom model remained stable during a follow-up period of 15 months. Recently, Marengo et al. (2000) observed stability of a four-dimensional factor model during a 10-year period, but found relative independence concerning the courses of individual symptom dimen-

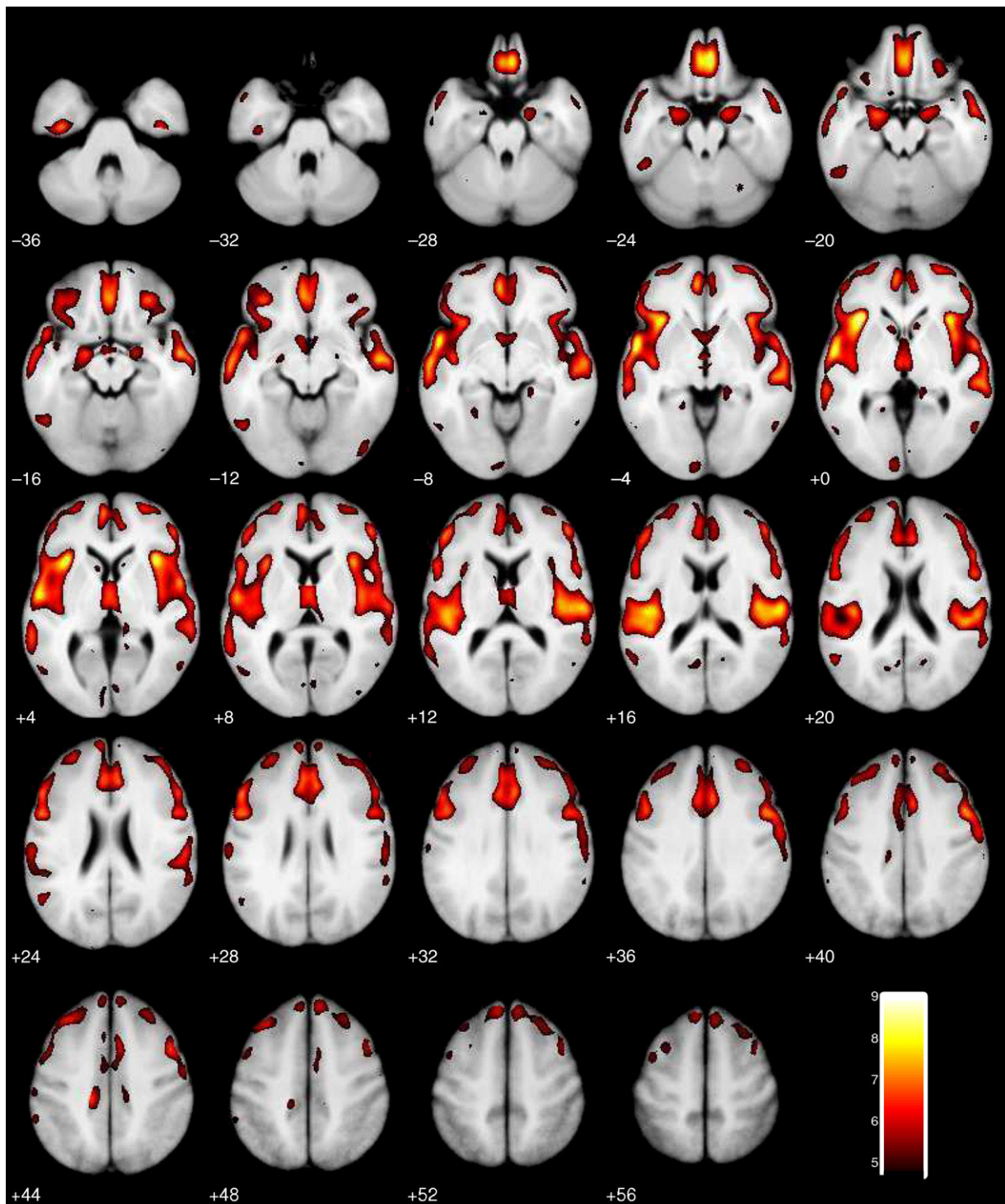


Fig. 1. Regions showing GMD losses in 175 SZ versus 177 HC ($p < 0.05$, FWE) after statistically correcting for age and gender effects.

sions. McGlashan (1998) showed that schizophrenic subtypes were relatively stable only during the first years of the clinical course and that changes occurred in the direction of more frequent negative and disorganized phenotypes. These data suggest stability of the described symptom dimensions during the first years of the disease process. Nevertheless, only longitudinal studies combining psychopathological and structural brain data collected over different

disease stages may validly investigate the temporal dynamics of clinical phenotypes and their structural brain correlates.

Whole-group VBM analysis

Regardless of the clinical diversity of our patient population, we found significant GMD reductions within the frontal, temporal,

	HC > SZ												HC > SZ-NEG												HC > SZ-POS												HC > SZ-DIS																	
	L						R						L						R						L						R																							
	k	T	P	x	y	z	k	T	P	x	y	z	k	T	P	x	y	z	k	T	P	x	y	z	k	T	P	x	y	z	k	T	P	x	y	z	k	T	P	x	y	z												
Perisylvian & Intrasylvian																																																						
Frontal Inferior Opercular	3169						4237						2015						3005						462						166	4.9	.020	57	8	21	220						62	4.84	.027	51	14	7						
Frontal Inferior Triangular	7118						4798						3022	7	.000	-54	22	27	2736	6.8	.000	54	24	24	1024	5.9	.000	-54	17	8	144						27						486											
Heschl	1399						1273																																															
Insula	9682	8.9	.000	-34	22	0	8207	8.4	.000	36	20	4	5161	7.2	.000	-34	22	-2	4384	7.1	.000	37	21	-1	1504	5.6	.001	-37	14	2	855	5.7	.001	39	9	0							1046	5.75	.000	36	20	4						
Parietal Inferior	305	5.3	.003	-58	-44	45																																																
Postcentral	1719						2293												1118						170												535																	
Precentral	2419						3334						1184						1285						387	5.3	.004	-55	8	29	476												2437	6.15	.000	55	-19	13						
Rolandic operculum	5034	8.3	.000	-55	-5	1	6606	7.7	.000	49	-18	14	1885						3414						2121	5.8	.000	-45	-21	18	1195	5.4	.003	55	3	5																		
Supramarginal	1557						2752						331						34	4.8	.032	66	-32	41	189						342	5.4	.003	57	-23	19																		
Temporal Pole Middle													417												71																													
Temporal Pole Superior	2011						1520						1790	7.4	.000	-54	7	-8	1277						2444	6.1	.000	-54	-4	0	96																							
Temporal Superior	10127	8.6	.000	-53	3	-5	10740						2880						5143	5.1	.010	63	-40	19																														
Temporal																																																						
Fusiform	607	7.3	.000	-37	-14	-38	396	6.4	.000	40	-14	-38	223	6.6	.000	-39	-11	-41	221	5.4	.002	41	-14	-38																														
Temporal Inferior	2368						322						917						194	4.8	.039	66	-42	-16																														
Temporal Middle	8815						4802	5.7	.001	56	-63	0	3501						4022	6.7	.000	56	-4	-17	139	5	.017	-64	-50	6																								
Frontal																																																						
Frontal Inferior Orbital	4393						2156						2081						1485						147	5.1	.009	-40	24	-16																								
Frontal Medial Orbital	2377	7.5	.000	-6	47	-8	2209						1248						769						438	5.3	.005	-4	44	-10																								
Frontal Middle	8138						8810						3305	4.9	.018	-29	11	58	6158						408						424	5.6	.001	47	9	40																		
Frontal Middle Orbital	1239						1205												519						22																													
Frontal Superior	2985	4.8	.028	-22	4	67	2683						1512	5	.015	-16	17	64	1770																																			
Frontal Superior Medial	7301						3741	5.5	.002	9	61	28	3274	6.3	.000	-5	55	3	721	4.8	.039	8	59	30																														
Frontal Superior Orbital																																																						
Rectus	3147	4.9	.024	-10	12	-21	2462	8.7	.000	4	38	-25	1983	6.9	.000	-4	35	-26	1739	7.5	.000	6	35	-26							65	5	.012	4	38	-25																		
Suppl. Motor Area	415						506						117	5	.013	-6	4	72																																				
Occipital																																																						
Calcarine	1283	5.8	.000	-8	-93	-1	313	5	.012	5	-81	5																																										
Cuneus	67	5	.012	-14	-66	21	40	5.1	.011	16	-59	19																																										
Lingual	297	5.2	.005	-18	-49	-2	155																																															
Occipital Inferior							396	5.8	.000	43	-81	-13																			213	5.3	.004	38	-87	-12																		
Occipital Middle							64	5	.014	40	-84	9																																										
Precuneus	190	5.2	.006	-6	-62	17	63	5	.017	13	-49	5																																										
Limbic																																																						
Amygdala	991	7	.000	-21	-5	-20	577						600	6.1	.000	-22	-5	-22	342						25	4.8	.039	-4	32	24	61	4.9	.023	8	35	23	194	5.19	.006	-21	-5	-17												
Cingulate Anterior	4076						3271						1821						1903																		281	5.13	.008	-4	35	26												
Hippocampus	1607	5.7	.000	-4	-3	-15	616	4.9	.024	30	-20	-14	509	4.7	.042	-4	-2	-13	577	6.5	.000	21	-4	-23							42	4.87	.024	-29	-19	-14																		
Cingulate Middle	3030	6.7	.000	-15	-30	45	3204	5.2	.006	13	-27	45	979	5.4	.002	-13	-29	45	1566						149	5.1	.007	9	14	42	338	5.55	.001	-16	-29	43																		
Parahippocampus	457	4.8	.038	-17	-40	-6	1050	6.3	.000	19	-4	-23	108						1021																																			
Thalamus & Basal ganglia																																																						
Caudate	748	6	.000	-5	6	-9	498						175	5.1	.008	-7	9	-9																																				
Thalamus	943						1355	6.8	.000	1	-7	6	248	5	.012	-2	-12	7							229	5.1	.009	-4	-12	-1	433	5.3	.003	5	-13	1																		
Cerebellum																																																						
Cerebellum 10	30	5.7	.001	-19	-37	-48																																																
Cerebellum 6							211	5.2	.007	27	-62	-23	97	4.9	.018	-21	-58	-23	285	5.3	.004	25	-59	-23																														
Cerebellum 8	45																																																					
Cerebellum 9	90																																																					
Voxel Sum	100179						86865						40966						46105						9986						4619						12068						8256											

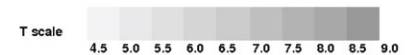


Fig. 2. Overview of VBM results. By means of AAL, suprathreshold voxels ($p < 0.05$, FWE corrected) were assigned to anatomical structures after evaluating GMD differences using the contrasts HC > SZ (white), HC > one (red), HC > SZ-POS (green), HC > SZ-DIS (blue box). The number of significant voxels (k) is listed for every structure, hemisphere (L/R) and contrast, if available. Additionally, for every cluster of significant voxels, the maximum number of three local voxel significance peaks was extracted by SPM and assigned to the corresponding anatomical structure by AAL with T and p values, as well as anatomical coordinates in

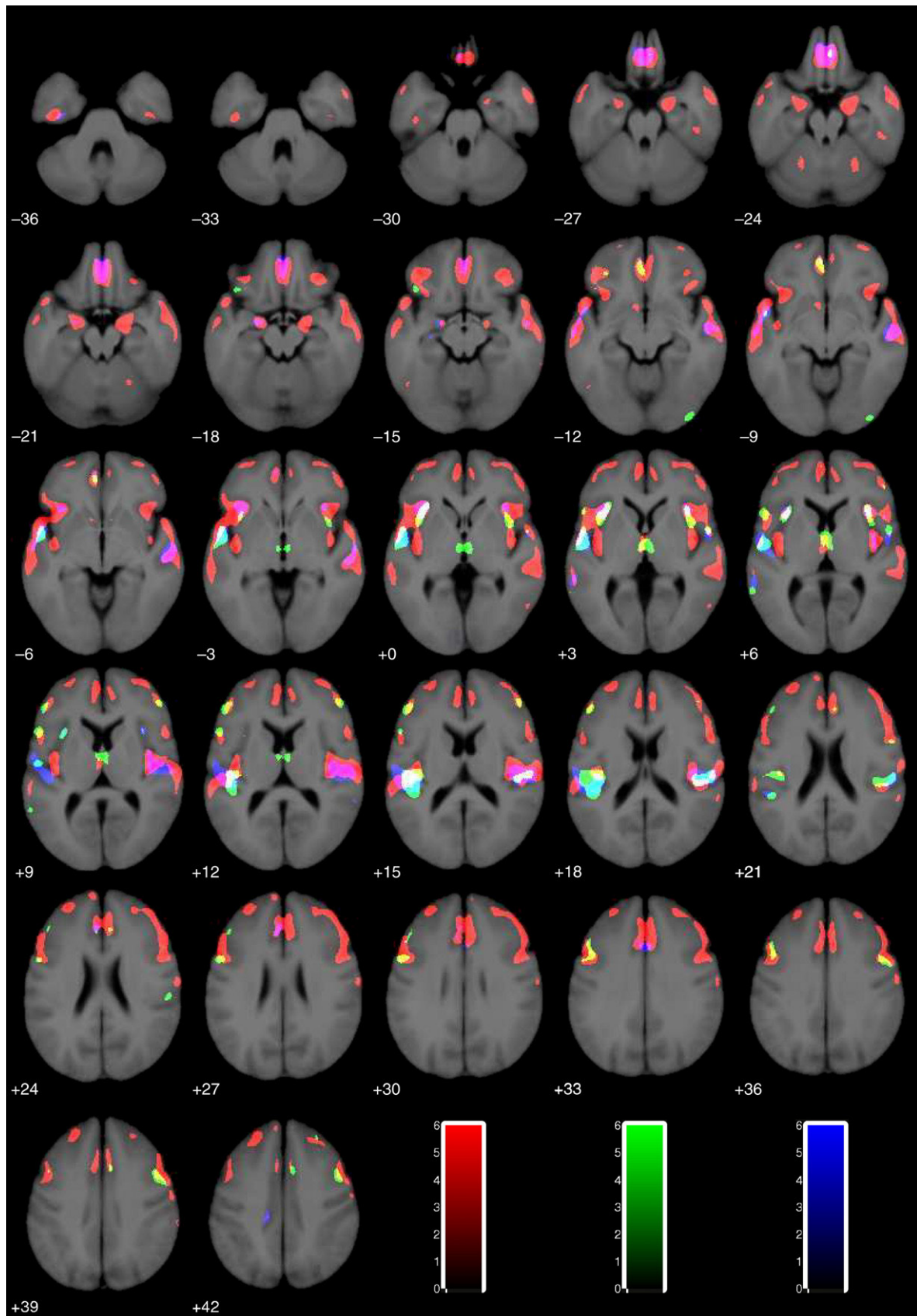


Fig. 3. Regions showing GMD losses in SZ-NEG (red), SZ-POS (green) and SZ-DIS (blue clusters) versus HC ($p < 0.05$, FWE) after statistically correcting for age and gender effects.

parietal and limbic lobes, as well as several subcortical structures of the entire SZ group compared to HC. The anatomical loci of our findings are consistent with a recent meta-analysis of 15 VBM studies (Honea et al., 2005). Over 30% of these studies reported alterations in the medial and lateral temporal lobe structures as well as in the inferior frontal and medial frontal cortices. In contrast to our bilateral perisylvian, limbic and paralimbic findings, a majority of VBM studies reported mainly left-hemispheric alterations for these regions. However, our observations agree with the to-date largest VBM study of 159 patients and 158 healthy control subjects (Hulshoff Pol et al., 2001) that identified primarily bilateral brain abnormalities. The inconsistencies regarding the laterality of findings may relate to highly divergent sample sizes or to different prevailing phenotypes across study populations.

Honea et al. (2005) listed also less frequently reported brain regions including the insular, anterior cingulate, orbitofrontal and parietal cortex, as well as subcortical structures (thalamus, caudate nucleus, cerebellum). In this context, the results of our whole-group analysis provide further support for significant structural alterations in these brain regions.

PANSS factor samples

The VBM analysis of the three factor samples identified selective patterns of structural differences between the symptom dimensions. We measured medium to large effect sizes for the suprathreshold voxels across all factors samples (Supplementary Figs. 3–5). Moreover, the supplementary VBM analysis revealed increasing structural differences in the GMD reduction patterns of high-loading versus low-loading subgroups compared to HC (Supplementary Figs. 9–11). Moreover, no significant interactions between GMD and age of onset and medication dose at scan time were found. Anatomical sample homogeneity was not significantly different between factor samples (Table 1).

SZ-NEG patients

This factor sample showed the most prominent and extended alterations affecting prefrontal, temporal, limbic and subcortical regions. In contrast to the other factor samples, SZ-NEG patients showed significant bilateral limbic and prefrontal GMD reductions.

Although our negative symptom dimension may not completely overlap with the definition of “deficit schizophrenia”, it matched important core items of this concept (Kirkpatrick et al., 2001). This model defines a separate clinical subtype of schizophrenia characterized by the presence of “primary and stable negative symptoms” leading to poorer social functioning already before and at the onset of psychosis. These deficit symptoms are consistent with core features of the negative symptom dimension including high factor loadings on PANSS items like “emotional withdrawal” or “blunted affect” reflecting social and emotional dysfunction.

The limbic system has been in the focus of neurobiological research in schizophrenia since earlier postmortem studies (Bogerts, 1997). Beside the established role of the hippocampus in mnemonic functions, the amygdala and other brain areas involved in emotional processing have received growing scientific attention, as they may subserve deficient affective processing in schizophrenic patients (Phillips et al., 2003). This “emotional brain” may include the anterior insula, the ACC, as well as medial prefrontal and temporal structures. Consistent with our findings, these regions have been repeatedly found to be altered in schizophrenia (Makris et al., 2006;

Shurman et al., 2005; Suzuki et al., 2005; Yücel et al., 2003; Sanfilipo et al., 2000).

Our results support the VBM study by Sigmundsson et al. (2001) that examined a clinically homogeneous group of 27 patients with enduring negative symptoms following the criteria for “deficit schizophrenia” (Kirkpatrick et al., 2001). These patients were additionally characterized by the PANSS, with scores nearby identical to our SZ-NEG sample. The authors detected GMD alterations within medial prefrontal, perisylvian, limbic and paralimbic brain areas compared to healthy volunteers. In contrast to our bilateral observations, their findings of perisylvian and paralimbic/limbic GMD reductions were primarily left-lateralized. However, the authors observed also right-sided GMD reductions in corresponding anatomical regions at a less stringent significance level. We could not replicate their results of GMD increments in several left-hemispheric subcortical structures (putamen, globus pallidus, nucleus accumbens) which previously have been attributed to hypertrophic effects of neuroleptic medication (Chakos et al., 1994). Instead, we identified left-hemispheric GMD reductions in the caudate nucleus and the thalamus.

Although a number of functional neuroimaging studies have consistently reported reduced DLPFC activations in cognitive tasks (Glahn et al., 2005), only few structural studies have been performed in deficit versus non-deficit patients with inconsistent results: Turetsky et al. (1995) reported smaller total prefrontal volumes in deficit versus non-deficit patients. In contrast, Buchanan et al. (1993) observed smaller prefrontal white matter volumes in non-deficit versus deficit patients. Taken together, our own findings of extended GMD reductions within the lateral prefrontal cortices, along with the medial prefrontal, perisylvian and limbic observations, support our hypothesis of a fronto-temporo-limbic pattern of structural alterations in this factor sample.

SZ-POS patients

In line with our hypothesis, this factor sample showed mainly left-lateralized structural alterations in language-related cortical areas and lateral prefrontal regions as well as the thalamus, bilaterally. These alterations did not reach the extent of the SZ-NEG group and did not, in contrast to our initial hypothesis, affect the limbic system. Thalamic GMD reductions were more pronounced compared to the other factor samples.

Previous studies using the SANS/SAPS scales reported high factor loadings for hallucinations and delusions (Arndt et al., 1991). However, we observed more “unspecific” symptoms like “hostility”, “excitement” and “guilt feelings” among the high-loading items of the positive symptom dimension. The mixture of general psychopathology items reflecting the acute psychotic state and “typical” positive symptoms may contribute to a higher phenotypical heterogeneity in this symptom dimension (Supplementary Fig. 12).

Alterations of the thalamic nuclei in schizophrenia have been investigated by a considerable number of neuroimaging studies (Sim et al., 2006). Some studies reported thalamic abnormalities in line with a potentially disturbed gating function of the thalamus and a disruption of normal information processing within thalamo-cortical networks. However, these results have been difficult to replicate as recent postmortem and MRI studies reported primarily negative results (Danos et al., 2005; Cullen et al., 2003; Bagary et al., 2002; Deicken et al., 2002). Our findings of extended thalamic GMD losses in patients with predominant positive symptoms may strengthen the hypothesis of thalamic dysfunction

in overt psychosis. However, more research is needed in order to elucidate the relationships between thalamic alterations and clinical parameters in schizophrenia.

Using ROI techniques, Barta et al. (1990) first described a correlation between volumetric STG alterations and auditory hallucinations in schizophrenic patients. Consistent with this finding, Flaum et al. (1995) showed a correlation between left-lateralized volumetric reductions of the STG and greater severity of hallucinations. Gaser et al. (2004) reported correlations between morphometric alterations of perisylvian and prefrontal structures and auditory hallucinations. Recently, Hubl et al. (2004) suggested a disconnection of the perisylvian language network as a substrate for hallucinatory behavior using DTI. Finally, all these findings including our own results are consistent with functional neuroimaging studies showing an impaired activation of temporal areas involved in the monitoring of inner speech (McGuire et al., 1995; Dierks et al., 1999).

To date, few correlation studies have investigated the links between delusional beliefs and morphometric brain alterations. Flaum et al. (1995) failed to find an inverse correlation between delusions and STG volume. Pressler et al. (2005) found a positive correlation between ROI measurements of the insula and the positive symptom dimension of their factor-analytic approach. However, within this symptom dimension, delusions and ROI measurements were not significantly correlated.

Up to now, there is only one VBM study available that, differently to our approach, examined a clinically homogeneous subgroup of 35 patients with paranoid schizophrenia (Ha et al., 2004). In comparison to our SZ-POS sample, the PANSS positive sum score of these patients attained comparable scores. Interestingly, our structural VBM findings fit very well to the results of Ha et al. (2004) that were localized to the medial prefrontal regions, the anterior cingulate and the perisylvian regions, as well as the dorsolateral prefrontal and insular cortex of the left hemisphere.

SZ-DIS patients

The GMD reductions in this factor sample were more extended than expected by our hypothesis and included the perisylvian structures, the middle temporal gyrus and the medial orbitofrontal cortex, bilaterally. Left-hemispheric alterations were identified in the medial temporal lobe structures (amygdala, hippocampus, parahippocampus) and the ACC.

The item distribution of the disorganized symptom dimension was consistent with many previous factor-analytic studies identifying a disorganized factor within three-, four- or five-factor models of schizophrenic psychopathology across highly heterogeneous patient populations (Van den Oord et al., 2006; von Knorring and Lindstrom, 1995; Bell et al., 1994a; Lindenmayer et al., 1994; Peralta and Cuesta, 1994; Arndt et al., 1991; Kay and Sevy, 1990). The internal consistency of the disorganized component was moderate, but in line with the studies of Bell et al. (1994a) and Kay and Sevy (1990). Moreover, previous reports showed a strong concurrent validity with established neuropsychological and neurological measures (Bryson et al., 1999; Bell et al., 1994b; Liddle and Morris, 1991; Liddle, 1987).

Bleuler (1911) related disorganized symptoms to a fundamental disturbance of thought processes. Due to the intimate connections between thought- and language-related processes, ROI investigations of schizophrenic patients have focused on the temporal lobe structures as the neural substrate of disorganized symptoms, but their findings are inconsistent: Shenton et al. (1992) observed an

inverse correlation between formal thought disorder (FTD) and volumetric losses in the left posterior STG. Rajarethinam et al. (2001) found a significant negative correlation between left-sided AHC volume and the severity of the BPRS item “conceptual disorganization”. However, a recent ROI study by Subotnik et al. (2003) failed to replicate these AHC findings using the BPRS and the Bizarre-Idiosyncratic Thinking Scale (BIZ). The authors reported bilateral inverse correlations between volume losses in the posterior STG and the BIZ scale. In contrast to these findings, Flaum et al. (1995) and Pressler et al. (2005) did not find any significant correlations between the disorganized symptom dimension and any ROI measurements including the STG and the insula.

Our VBM results in this symptom dimension may point to structural alterations within a cortical network that may form a neural substrate of FTD and disorganized symptoms (Goldberg et al., 1998; Aloia et al., 1998). This network involves the perisylvian structures, the parahippocampus, the DLPFC and ACC as well as the inferior parietal cortex. Recent fMRI studies have shown deficient activation patterns in these structures during the processing of semantic information and object recall stimuli in schizophrenic patients (Assaf et al., 2006; Kircher et al., 2002; McGuire et al., 1998).

Structural correlates of psychopathological symptom dimensions

In view of the considerable clinical and neurobiological heterogeneity, it is still a matter of debate whether schizophrenia represents a clinical syndrome rather than a single disease entity (Andreasen, 2000). In the 1980s, this debate was inspired by the “positive-negative” dichotomy (Crow, 1980) that distinguished type-I from type-II schizophrenia. Later on, the dichotomy was criticized for not capturing the full syndromal structure of the disease (Arndt et al., 1991). Hence, “disorganization” was introduced as third syndromal cluster based on converging results from different factor-analytic studies (Grube et al., 1998). External validity to this model was provided by several neuropsychological and neurobiological investigations (Harris et al., 1999; Bryson et al., 1999; Bell et al., 1994b; Liddle and Morris, 1991). Nevertheless, Andreasen et al. (1995) and Arndt et al. (1995) reconsidered schizophrenic symptomatology from a dimensional point of view, regarding independent, but overlapping and coexisting symptom dimensions as the constituents of the disease’s phenotypical diversity.

What contribution may our data make to this ongoing debate? Comparison of the three PANSS factor samples versus the healthy control group revealed selective patterns of structural alterations associated with the negative, positive and disorganized symptom dimension. However, the percental differences *between* the factor samples were subtle compared to the size of GMD differences between HC and the entire SZ group (Supplementary Figs. 2 and 6). Moreover, the conjunctive analysis identified a considerable overlap of GMD reduction patterns among the factor samples. In this context, the delineation of relatively “pure” phenotypes in our supplementary VBM analysis (Supplementary Figs. 9–11) increased the *between*-factor differences, possibly by reducing the remaining phenotypical and structural heterogeneity within the factor groups. This heterogeneity may be determined by a number of important limitations, including (1) the methodology of VBM (see Davatzikos, 2004, and Bookstein, 2001, for critical comments), (2) different measurability, sensitivity and specificity of the PANSS items, (3) our factor-analytic approach (numbers of factors) and (4)

the clinical state of the patients (acute versus remitted, first-episode versus chronic patients).

In summary, our results describe a pattern of structural alterations within the prefrontal, perisylvian, temporal, limbic and subcortical brain regions based on the MRI data of a large and heterogeneous patient group compared to a matched healthy control group. The approach of combining VBM with factor analysis of psychopathological measurements revealed selective structural correlates of negative, positive and disorganized symptom dimensions. The differences between these correlates indicate that the structural heterogeneity in schizophrenia may relate to the phenotypical diversity of the disease. Conjunctive analysis identified a significant overlap between these structural correlates suggesting a unifying pattern of alterations inherent in all symptom clusters. In the future, further cross-sectional and longitudinal replication studies are needed in order to quantify the extent of structural differences and overlaps between the different symptom dimensions of schizophrenia.

Appendix A. Supplementary data

Supplementary data associated with this article can be found, in the online version, at [doi:10.1016/j.neuroimage.2007.10.029](https://doi.org/10.1016/j.neuroimage.2007.10.029).

References

- Aloia, M.S., Gourovitch, M.L., Missar, D., Pickar, D., Weinberger, D.R., Goldberg, T.E., 1998. Cognitive substrates of thought disorder: II. Specifying a candidate cognitive mechanism. *Am. J. Psychiatry* 155 (12), 1677–1684.
- Andreasen, N.C., Arndt, S., Alliger, R., Miller, D., Flaum, M., 1995. Symptoms of schizophrenia. Methods, meanings, and mechanisms. *Arch. Gen. Psychiatry* 52 (5), 341–351.
- Andreasen, N.C., 1999. A unitary model of schizophrenia: Bleuler's "fragmented phrene" as schizencephaly. *Arch. Gen. Psychiatry* 56 (9), 781–787.
- Andreasen, N.C., 2000. Schizophrenia: the fundamental questions. *Brain Res. Brain Res. Rev.* 31 (2–3), 106–112.
- Arndt, S., Alliger, R.J., Andreasen, N.C., 1991. The distinction of positive and negative symptoms. The failure of a two-dimensional model. *Br. J. Psychiatry* 158, 317–322.
- Arndt, S., Andreasen, N.C., Flaum, M., Miller, D., Nopoulos, P., 1995. A longitudinal study of symptom dimensions in schizophrenia. Prediction and patterns of change. *Arch. Gen. Psychiatry* 52 (5), 352–360.
- Assaf, M., Rivkin, P.R., Kuzu, C.H., Calhoun, V.D., Kraut, M.A., Groth, K.M., Yassa, M.A., Hart, J., Pearlson, G.D., 2006. Abnormal object recall and anterior cingulate overactivation correlate with formal thought disorder in schizophrenia. *Biol. Psychiatry* 59 (5), 452–459.
- Bach Cuadra, M., Cammoun, L., Butz, T., Cuisenaire, O., Thiran, J.-P., 2005. Comparison and validation of tissue modelization and statistical classification methods in T1-weighted MR brain images. *IEEE Trans. Med. Imag.* 24 (12), 1548–1565.
- Bagary, M.S., Foong, J., Maier, M., duBoulay, G., Barker, G.J., Miller, D.H., Ron, M.A., 2002. A magnetization transfer analysis of the thalamus in schizophrenia. *J. Neuropsychiatry Clin. Neurosci.* 14 (4), 443–448.
- Barta, P.E., Pearlson, G.D., Powers, R.E., Richards, S.S., Tune, L.E., 1990. Auditory hallucinations and smaller superior temporal gyral volume in schizophrenia. *Am. J. Psychiatry* 147 (11), 1457–1462.
- Bell, M.D., Lysaker, P.H., Beam-Goulet, J.L., Milstein, R.M., Lindenmayer, J.P., 1994a. Five-component model of schizophrenia: assessing the factorial invariance of the positive and negative syndrome scale. *Psychiatry Res.* 52 (3), 295–303.
- Bell, M.D., Lysaker, P.H., Milstein, R.M., Beam-Goulet, J.L., 1994b. Concurrent validity of the cognitive component of schizophrenia: relationship of PANSS scores to neuropsychological assessments. *Psychiatry Res.* 54 (1), 51–58.
- Bleuler, E., 1911. *Dementia Praecox oder Gruppe der Schizophrenien*. Leipzig, Wien, Deuticke.
- Bogerts, B., 1997. The temporolimbic system theory of positive schizophrenic symptoms. *Schizophr. Bull.* 23 (3), 423–435.
- Bookstein, F.L., 2001. "Voxel-based morphometry" should not be used with imperfectly registered images. *NeuroImage* 14 (6), 1454–1462.
- Bryson, G., Bell, M., Greig, T., Kaplan, E., 1999. Internal consistency, temporal stability and neuropsychological correlates of three cognitive components of the positive and negative syndrome scale (PANSS). *Schizophr. Res.* 38 (1), 27–35.
- Buchanan, R.W., Breier, A., Kirkpatrick, B., Elkashef, A., Munson, R.C., Gellad, F., Carpenter, W.T., 1993. Structural abnormalities in deficit and nondeficit schizophrenia. *Am. J. Psychiatry* 150 (1), 59–65.
- Carpenter, W.T., Heinrichs, D.W., Wagman, A.M., 1988. Deficit and non-deficit forms of schizophrenia: the concept. *Am. J. Psychiatry* 145 (5), 578–583.
- Chakos, M.H., Lieberman, J.A., Bilder, R.M., Borenstein, M., Lerner, G., Bogerts, B., Wu, H., Kinon, B., Ashtari, M., 1994. Increase in caudate nuclei volumes of first-episode schizophrenic patients taking antipsychotic drugs. *Am. J. Psychiatry* 151 (10), 1430–1436.
- Crespo-Facorro, B., Kim, J., Andreasen, N.C., O'Leary, D.S., Bockholt, H.J., Magnotta, V., 2000. Insular cortex abnormalities in schizophrenia: a structural magnetic resonance imaging study of first-episode patients. *Schizophr. Res.* 46 (1), 35–43.
- Crespo-Facorro, B., Nopoulos, P.C., Chemerinski, E., Kim, J.-J., Andreasen, N.C., Magnotta, V., 2004. Temporal pole morphology and psychopathology in males with schizophrenia. *Psychiatry Res.* 132 (2), 107–115.
- Crow, T.J., 1980. Positive and negative schizophrenic symptoms and the role of dopamine. *Br. J. Psychiatry* 137, 383–386.
- Cullen, T.J., Walker, M.A., Parkinson, N., Craven, R., Crow, T.J., Esiri, M.M., Harrison, P.J., 2003. A postmortem study of the mediodorsal nucleus of the thalamus in schizophrenia. *Schizophr. Res.* 60 (2–3), 157–166.
- Danos, P., Schmidt, A., Baumann, B., Bernstein, H.-G., Northoff, G., Stauch, R., Krell, D., Bogerts, B., 2005. Volume and neuron number of the mediodorsal thalamic nucleus in schizophrenia: a replication study. *Psychiatry Res.* 140 (3), 281–289.
- Davatzikos, C., Shen, D., Gur, R.C., Wu, X., Liu, D., Fan, Y., Hughett, P., Turetsky, B.I., Gur, R.E., 2005. Whole-brain morphometric study of schizophrenia revealing a spatially complex set of focal abnormalities. *Arch. Gen. Psychiatry* 62 (11), 1218–1227.
- Davatzikos, C., 2004. Why voxel-based morphometric analysis should be used with great caution when characterizing group differences. *NeuroImage* 23 (1), 17–20.
- Deicken, R.F., Eliaz, Y., Chosiad, L., Feiwell, R., Rogers, L., 2002. Magnetic resonance imaging of the thalamus in male patients with schizophrenia. *Schizophr. Res.* 58 (2–3), 135–144.
- Dierks, T., Linden, D.E., Jandl, M., Formisano, E., Goebel, R., Lanfermann, H., Singer, W., 1999. Activation of Heschl's gyrus during auditory hallucinations. *Neuron* 22 (3), 615–621.
- Flaum, M., O'Leary, D.S., Swayze, V.W., Miller, D.D., Arndt, S., Andreasen, N.C., 1995. Symptom dimensions and brain morphology in schizophrenia and related psychotic disorders. *J. Psychiatr. Res.* 29 (4), 261–276.
- Friston, K.J., Penny, W.D., Glaser, D.E., 2005. Conjunction revisited. *NeuroImage* 25 (3), 661–667.
- Gaser, C., Nenadic, I., Volz, H.-P., Buchel, C., Sauer, H., 2004. Neuroanatomy of "hearing voices": a frontotemporal brain structural abnormality associated with auditory hallucinations in schizophrenia. *Cereb. Cortex* 14 (1), 91–96.
- Gaser, C., Volz, H.P., Kiebel, S., Riehemann, S., Sauer, H., 1999. Detecting structural changes in whole brain based on nonlinear deformations—application to schizophrenia research. *NeuroImage* 10 (2), 107–113.

- Glahn, D.C., Ragland, J.D., Abramoff, A., Barrett, J., Laird, A.R., Bearden, C.E., Velligan, D.I., 2005. Beyond hypofrontality: a quantitative meta-analysis of functional neuroimaging studies of working memory in schizophrenia. *Hum. Brain Mapp.* 25 (1), 60–69.
- Goldberg, T.E., Aloia, M.S., Gourovitch, M.L., Missar, D., Pickar, D., Weinberger, D.R., 1998. Cognitive substrates of thought disorder: I. The semantic system. *Am. J. Psychiatry* 155 (12), 1671–1676.
- Good, C.D., Johnsrude, I.S., Ashburner, J., Henson, R.N., Friston, K.J., Frackowiak, R.S., 2001. A voxel-based morphometric study of ageing in 465 normal adult human brains. *NeuroImage* 14 (1 Pt. 1), 21–36.
- Grube, B.S., Bilder, R.M., Goldman, R.S., 1998. Meta-analysis of symptom factors in schizophrenia. *Schizophr. Res.* 31 (2–3), 113–120.
- Ha, T.H., Y., T., Ha, K.S., Rho, K.S., Lee, J.M., Kim, I.Y., Kim, S.I., Kwon, J.S., 2004. Gray matter abnormalities in paranoid schizophrenia and their clinical correlations. *Psychiatry Res.* 132 (3), 251–260.
- Harris, A.W., Williams, L., Gordon, E., Bahramali, H., Slewa-Younan, S., 1999. Different psychopathological models and quantified EEG in schizophrenia. *Psychol. Med.* 29 (5), 1175–1181.
- Honea, R., Crow, T.J., Passingham, D., Mackay, C.E., 2005. Regional deficits in brain volume in schizophrenia: a meta-analysis of voxel-based morphometry studies. *Am. J. Psychiatry* 162 (12), 2233–2245.
- Hubl, D., Koenig, T., Strik, W., Federspiel, A., Kreis, R., Boesch, C., Maier, S.E., Schroth, G., Lovblad, K., Dierks, T., 2004. Pathways that make voices: white matter changes in auditory hallucinations. *Arch. Gen. Psychiatry* 61 (7), 658–668.
- Hulshoff Pol, H.E., Schnack, H.G., Mandl, R.C., van Haren, N.E., Koning, H., Collins, D.L., Evans, A.C., Kahn, R.S., 2001. Focal gray matter density changes in schizophrenia. *Arch. Gen. Psychiatry* 58 (12), 1118–1125.
- Kay, S.R., Fiszbein, A., Opler, L.A., 1987. The positive and negative syndrome scale (PANSS) for schizophrenia. *Schizophr. Bull.* 13 (2), 261–276.
- Kay, S.R., Sevy, S., 1990. Pyramidal model of schizophrenia. *Schizophr. Bull.* 16 (3), 537–545.
- Kircher, T.T.J., Liddle, P.F., Brammer, M.J., Williams, S.C.R., Murray, R.M., McGuire, P.K., 2002. Reversed lateralization of temporal activation during speech production in thought disordered patients with schizophrenia. *Psychol. Med.* 32 (3), 439–449.
- Kirkpatrick, B., Buchanan, R.W., Ross, D.E., Carpenter, W.T., 2001. A separate disease within the syndrome of schizophrenia. *Arch. Gen. Psychiatry* 58 (2), 165–171.
- Lambert, M., Moritz, S., Naber, D., 2004. Pharmakotherapie der Schizophrenie. In: Naber, D., Lambert, M. (Eds.), *Schizophrenie*. Georg Thieme Verlag, Stuttgart, New York, pp. 69–106.
- Liddle, P.F., 1987. The symptoms of chronic schizophrenia. A re-examination of the positive-negative dichotomy. *Br. J. Psychiatry* 151, 145–151.
- Liddle, P.F., Morris, D.L., 1991. Schizophrenic syndromes and frontal lobe performance. *Br. J. Psychiatry* 158, 340–345.
- Lindenmayer, J.P., Bernstein-Hyman, R., Grochowski, S., 1994. Five-factor model of schizophrenia. Initial validation. *J. Nerv. Ment. Dis.* 182 (11), 631–638.
- Makris, N., Goldstein, J.M., Kennedy, D., Hodge, S.M., Caviness, V.S., Faraone, S.V., Tsuang, M.T., Seidman, L.J., 2006. Decreased volume of left and total anterior insular lobule in schizophrenia. *Schizophr. Res.* 83 (2–3), 155–171.
- Marengo, J., Harrow, M., Herbener, E.S., Sands, J., 2000. A prospective longitudinal 10-year study of schizophrenia's three major factors and depression. *Psychiatry Res.* 97 (1), 61–77.
- Matsumoto, H., Simmons, A., Williams, S., Hadjulis, M., Pipe, R., Murray, R., Frangou, S., 2001. Superior temporal gyrus abnormalities in early-onset schizophrenia: similarities and differences with adult-onset schizophrenia. *Am. J. Psychiatry* 158 (8), 1299–1304.
- McGlashan, T.H., 1998. The profiles of clinical deterioration in schizophrenia. *J. Psychiatr. Res.* 32 (3–4), 133–141.
- McGuire, P.K., Quedest, D.J., Spence, S.A., Murray, R.M., Frith, C.D., Liddle, P.F., 1998. Pathophysiology of 'positive' thought disorder in schizophrenia. *Br. J. Psychiatry* 173, 231–235.
- McGuire, P.K., Silbersweig, D.A., Wright, I., Murray, R.M., David, A.S., Frackowiak, R.S., Frith, C.D., 1995. Abnormal monitoring of inner speech: a physiological basis for auditory hallucinations. *Lancet* 346 (8975), 596–600.
- Mesulam, M., Mufson, E., 1986. The insula of reil in man and monkey: architectonics, connectivity, and function. In: Peters, A., Jones, E.G. (Eds.), *Cereb. Cortex*. Plenum Press, New York, NY, pp. 179–226.
- Peralta, V., Cuesta, M.J., 1994. Psychometric properties of the positive and negative syndrome scale (PANSS) in schizophrenia. *Psychiatry. Res.* 53 (1), 31–40.
- Phillips, M.L., Drevets, W.C., Rauch, S.L., Lane, R., 2003. Neurobiology of emotion perception: II. Implications for major psychiatric disorders. *Biol. Psychiatry* 54 (5), 515–528.
- Pressler, M., Nopoulos, P., Ho, B.-C., Andreasen, N.C., 2005. Insular cortex abnormalities in schizophrenia: relationship to symptoms and typical neuroleptic exposure. *Biol. Psychiatry* 57 (4), 394–398.
- Rajarethinam, R., DeQuardo, J.R., Miedler, J., Arndt, S., Kirbat, R., Brunberg, J.A., Tandon, R., 2001. Hippocampus and amygdala in schizophrenia: assessment of the relationship of neuroanatomy to psychopathology. *Psychiatry Res.* 108 (2), 79–87.
- Sanfilippo, M., Lafargue, T., Rusinek, H., Arena, L., Loneragan, C., Lautin, A., Feiner, D., Rotrosen, J., Wolkin, A., 2000. Volumetric measure of the frontal and temporal lobe regions in schizophrenia: relationship to negative symptoms. *Arch. Gen. Psychiatry* 57 (5), 471–480.
- Schlösser, R., Gesierich, T., Kaufmann, B., Vucurevic, G., Hunsche, S., Gawehn, J., Stoeter, P., 2003. Altered effective connectivity during working memory performance in schizophrenia: a study with fMRI and structural equation modeling. *NeuroImage* 19 (3), 751–763.
- Shenton, M.E., Dickey, C.C., Frumin, M., McCarley, R.W., 2001. A review of MRI findings in schizophrenia. *Schizophr. Res.* 49 (1–2), 1–52.
- Shenton, M.E., Kikinis, R., Jolesz, F.A., Pollak, S.D., LeMay, M., Wible, C.G., Hokama, H., Martin, J., Metcalf, D., Coleman, M., 1992. Abnormalities of the left temporal lobe and thought disorder in schizophrenia. A quantitative magnetic resonance imaging study. *N. Engl. J. Med.* 327 (9), 604–612.
- Shurman, B., Horan, W.P., Nuechterlein, K.H., 2005. Schizophrenia patients demonstrate a distinctive pattern of decision-making impairment on the Iowa gambling task. *Schizophr. Res.* 72 (2–3), 215–224.
- Sigmundsson, T., Suckling, J., Maier, M., Williams, S., Bullmore, E., Greenwood, K., Fukuda, R., Ron, M., Toone, B., 2001. Structural abnormalities in frontal, temporal, and limbic regions and interconnecting white matter tracts in schizophrenic patients with prominent negative symptoms. *Am. J. Psychiatry* 158 (2), 234–243.
- Sim, K., Cullen, T., Ongur, D., Heckers, S., 2006. Testing models of thalamic dysfunction in schizophrenia using neuroimaging. *J. Neural Transm.* 113 (7), 907–928.
- Subotnik, K.L., Bartzokis, G., Green, M.F., Nuechterlein, K.H., 2003. Neuroanatomical correlates of formal thought disorder in schizophrenia. *Cognit. Neuropsychiatry* 8 (2), 81–88.
- Suzuki, M., Zhou, S.Y., Hagino, H., Niu, L., Takahashi, T., Kawasaki, Y., Matsui, M., Seto, H., Ono, T., Kurachi, M., 2005. Morphological brain changes associated with Schneider's first-rank symptoms in schizophrenia: a MRI study. *Psychol. Med.* 35 (4), 549–560.
- Turetsky, B.I., Cowell, P.E., Gur, R.C., Grossman, R.I., Shtasel, D.L., Gur, R.E., 1995. Frontal and temporal lobe brain volumes in schizophrenia. Relationship to symptoms and clinical subtype. *Arch. Gen. Psychiatry* 52 (12), 1061–1070.
- Tzourio-Mazoyer, N., Landeau, B., Papathanassiou, D., Crivello, F., Etard, O., Delcroix, N., Mazoyer, B., Joliot, M., 2002. Automated anatomical labeling of activations in SPM using a macroscopic anatomical parcellation of the MNI MRI single-subject brain. *NeuroImage* 15 (1), 273–289.
- Van den Oord, E.J.C.G., Rujescu, D., Robles, J.R., Giegling, I., Birrell, C., Buzsá, J., Murrelle, L., Möller, H.-J., Middleton, L., Muglia, P., 2006. Factor structure and external validity of the PANSS revisited. *Schizophr. Res.* 82 (2–3), 213–223.
- Van der Does, A.J.W., Dingemans, P.M., Linszen, D.H., Nugter, M.A.,

- Scholte, W.F., 1995. Dimensions and subtypes of recent-onset schizophrenia. A longitudinal analysis. *J. Nerv. Ment. Dis.* 183 (11), 681–687.
- Volz, H., Gaser, C., Sauer, H., 2000. Supporting evidence for the model of cognitive dysmetria in schizophrenia—a structural magnetic resonance imaging study using deformation-based morphometry. *Schizophr. Res.* 46 (1), 45–56.
- von Knorring, L., Lindström, E., 1995. Principal components and further possibilities with the PANSS. *Acta. Psychiatr. Scand. Suppl.* 388, 5–10.
- Wright, I.C., Rabe-Hesketh, S., Woodruff, P.W., David, A.S., Murray, R.M., Bullmore, E.T., 2000. Meta-analysis of regional brain volumes in schizophrenia. *Am. J. Psychiatry* 157 (1), 16–25.
- Yücel, M., Wood, S.J., Fornito, A., Riffkin, J., Velakoulis, D., Pantelis, C., 2003. Anterior cingulate dysfunction: implication for psychiatric disorders? *Rev. Psychiatr. Neurosci.* 28 (5), 350–354.